COMPUTATIONAL METHODS IN APPLIED MATHEMATICS, Vol. 8 (2008), No. 3, pp. 263–278

TOMOGRAPHIC APPROACH FOR TROPOSPHERIC WATER VAPOR DETECTION

P. MIIDLA[1], K. RANNAT[2], AND P. UBA[3]

Abstract — The technical successes in radio navigation and the availability of numerical algorithms have promoted the implementation of GPS-technology to atmospheric sciences. The tomographical contribution of Global Satellite Navigation Systems (GNSS) is possible due to the methods of high precision detection of tropospheric delays of navigation signals from satellites to receivers. The principal specific character in initial constraints, data collection and assimilation methods, the obtaining of final numerical results and their interpretation make the continuation of the success story for GPS-tomography very challenging. The authors use numerical simulation as the most time- and cost-efficient way to study different processes related to tropospheric water vapor tomography. This paper tends to give a short overview about some known methods in GPS-tomography for detection, monitoring and modeling of the tropospheric water vapor. The possible mathematical approach to the construction of virtual network of ground-based sensors (GPS-receivers) for a real geographical location and discretization of the troposphere, also some aspects of raw data filtering and analysis are described. Output of tomographical modelling of the troposphere can be used to improve the results of large-scale numerical weather prediction models and also real-time navigation. The questions of voxel geometry and methods of data processing are supposed to be the key questions in constructing an effective network of GPS-receivers for water vapor tomography.

2000 Mathematics Subject Classification: 86A10.
Keywords: Global Satellite Navigation System, troposphere, water vapor, GPS-tomography, Kalman filter.

1. Introduction

The GNSS (Global Satellite Navigation System known as GPS, GLONASS and further coming GALILEO) has become a part of everyday life. A lot of effort has been made to use navigation signals for obtaining information on the atmospheric properties on the satellite — ground-based receiver path. The GPS-signal is used, in particular, to obtain information on the concentration of tropospheric water vapor as one of the most important greenhouse gas and a carrier of latent heat in the atmosphere. Related large-scale experiments and monitoring have been launched in Japan (GEONET), US (SuomiNet), Europe (E-GVAP), etc.

Tomographic methods have been developed to get a 3D distribution of water vapor in the troposphere [5, 11, 14, 25]. The work on improvement and efficiency of the tomographic

[1] *Institute of Mathematics, University of Tartu*, J. Liivi 2, 50409 Tartu, Estonia. E-mail: peep.miidla@ut.ee
[2] *Institute of Automatics, Tallinn University of Technology*, Ehitajate tee 5, 12618 Tallinn, Estonia. E-mail: rannat@cs.ioc.ee
[3] *Estonian National Defence College*, Riia 12, 51013 Tartu, Estonia. E-mail: peep.uba@ksk.edu.ee

methods, largely depending on the experimental setup and mathematical methods is a part of interest and a subject of research for the Estonian group, partly presented at EMSS 2005 [23], Marseille. Special efforts are made to implement the Slant Delays and observation operator developed by R. Eresmaa and H. Järvinen at the Finnish Meteorological Institute (FMI) [10].

Although not so widely used yet, the tomographic method based on Slant Total Delay (STD) [36] has several essential advantages compared to traditional integrated precipitable water (IPW) estimation based on the Zenith Total Delay (ZTD) approach [30]. For high-resolution numerical weather prediction (NWP) the benefit of using STD is coming from the three main aspects: (i) the larger amount (of the order of 10) of observations available, as there are several satellites simultaneously visible from each point of observation, (ii) STD-observations can contain information on atmospheric anisotropy — temperature and humidity gradients (ZTD observations assume isotropic atmosphere), (iii) ZTD can be considered as a special case of STD (ZTD is derived from raw measurements along the slanted signal paths) [10]. The general scheme of information flows in GPS-tomography is shown in Fig. 1.1.

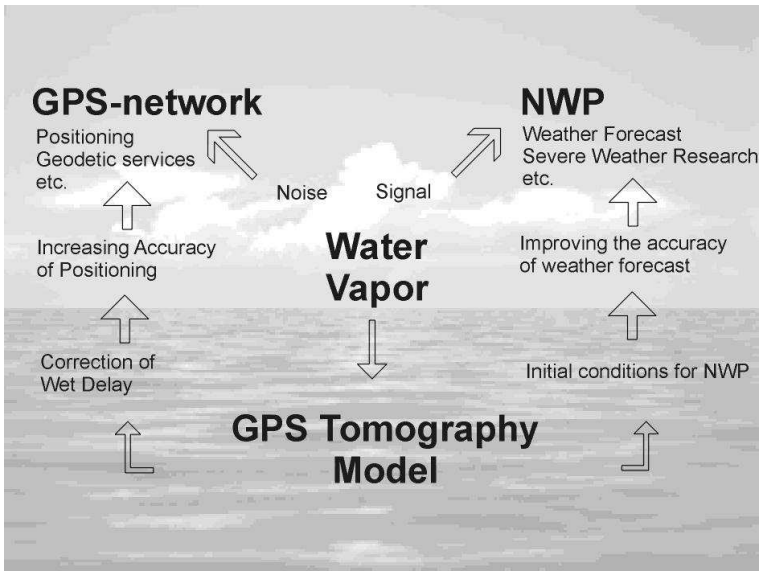

Fig. 1.1. Meteorological information from GPS navigation data

STD observations provide a potential for water vapor tomography – to obtain the real 3D distribution of tropospheric water for kilometric scale modeling, but on the other hand, the procedure for production of STD observations is still in the stage of evolution [9, 10]. It is not persuasively clear if the accuracy of near real time STD observations is adequate for the operational demands of NWP systems. Due to the geometry of the slanted signal paths, assimilation of STD is not as straightforward as the assimilation of ZTD. Moreover, it is currently not known how to properly account for the complicated observation error correlations of STD [10].

From the NWP point of view, ZTD is a desirable observation since it is a linear function of vertically Integrated Precipitable Water (IPW) above the GPS receiver [1]. IPW is directly related to the model humidity variable and is ideally suited to the model geometry. The relative complexity of usage of the slanted signal paths and common practice with NWP has suppressed the applicability of water vapor tomography at operational level. However, it rises challenges for research and modeling at present and in the future.

The first goal is to simulate a large-scale experiment (using a ground-based GPS receiver network). The situation is modelled where the information on the water vapor content surveillance is obtained from the ground-based GPS-receivers supported by additional meteorological sensors. These can be considered as stand-alone proactive agents with individual environment-dependent inputs and outputs. The information is processed by the central server and the results will be interpreted for the whole area of interest. The IPW from a fixed geographical position is obtained by GAMIT/GLOBK software (GAMIT/GLOBK is a GPS analysis package developed at Massachusetts Institute of Technology and Scripps Institution of Oceanography for the estimation of three-dimensional relative positions of ground stations and satellite orbits) and used as one of the links between simulation and reality. The real data from a fixed point are essential for calibration and evaluation of the model.

Kalman Filtering (KF) (and its modifications) has been investigated to minimize the noise in the initial data. The conventional KF is known as a serious computing power-consuming procedure for large sensor networks. The first results with real data for calibration were obtained and presented on December 2006.

2. Water vapor tomography – how it works

GPS signals propagating from GPS satellites to the receivers on the ground are affected by the atmosphere. Atmospheric refraction induces *slant delays* in individual rays propagating from GPS satellites to ground-based receivers. A Slant delay is expressed in terms of the excess path length of GPS radio signals along their propagation path between a GPS satellite and a ground-based receiver. The ionosphere has a dispersive effect on the GPS-frequencies (L1=1575.42 MHz, L2=1227.60 MHz) and the troposphere has a nondispersive effect on the GPS-signal. This allows the ionospheric effects to be removed by a linear combination of dual frequency data [18, 38]. The troposphere is a nondispersive medium and its impact cannot be determined by using the 2-frequency techniques.

In general, the effect of both the ionosphere and the troposphere can be measured by additional delays of the signal on the receiver-satellite path. Due to the atmospheric refraction the signal path is not the shortest straight line between receiver and satellite, but some kind of curve (Fig. 2.1).

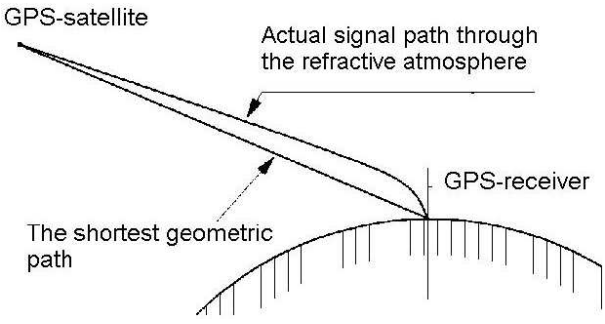

F i g. 2.1. Path of the radio signal through the atmosphere

On the path to the receiver, different components of the GPS-signal will arrive at the antenna at a different time instant. The ionospheric refraction causes a delay of the information package (modulated on the carrier signal) and the advance of the carrier phase. The physical reason is that the wave group and the phase velocity depend on the refraction index of the environment. Analysis, determination, and elimination of ionospheric effects are out of the scope of this article. A more detailed description can be found in [18, 20, 38].

The ionospheric delay can be removed (in the model case by adding supporting 2-band receivers to the monitoring network and interpolation of the ionospheric constituents between gridpoints).

The molecules of tropospheric gases and hydrometeors have a negative effect on the signal

propagation: increasing the noise component in the GPS-receiver and absorbing the signal. In most cases the absorption is not a trouble for GPS-networks. Atmospheric attenuation at GPS frequencies is of the order of 0.035 dB for a satellite in zenith and about 10 times more at low elevation angles. The attenuation is caused mainly by oxygen. The effects of water vapor, rain and nitrogen are negligible. Even a dense rainfall causes an attenuation less than 0.01 dB/km [29].

The delay caused by the neutral atmosphere can be divided into two components: zenith hydrostatic delay ("dry" component, ZHD) as a result of the induced dipole moment and zenith wet delay ("wet" component, ZWD) due to the permanent dipole moment of PW (Precipitable Water, water molecule) and liquid water (LW) present in the troposphere [31]. The wet component is spatially and temporally varying, therefore the errors in the models for the wet component are larger than the errors in the models for the "dry" component.

3. Delay of electromagnetic waves in the atmosphere

The general scheme of propagation of the electromagnetic signal through the atmosphere is shown in Fig. 2.1. Due to the refraction the actual path of a signal from the satellite to the receiver is longer than the shortest geometrical way.

The Slant total delay (STD) is induced by both dry air and water vapor. The Slant dry delay can be estimated by surface pressure measurements or by numerical weather models [6]. The Slant wet delay (SWD) can be estimated as the difference between the full slant delay and the slant dry delay. The tropospheric delay can be given as follows [18]:

$$\triangle^{trop} = \int n \cdot ds - \int ds = \int (n-1) ds \tag{3.1}$$

where $n(s)$ denotes the atmospheric refraction index on the signal path. Integration is performed over the total path in the troposphere and instead of the refractive index a new quantity $N^{trop} = 10^6(n-1)$ is introduced, because the numerical value of $(n-1)$ in the atmosphere is approximately 10^{-6}, therefore it is reasonable to multiply it by 10^6. Now N^{trop} varies from 0 to 300 and is often referred to as refraction. Equation (3.1) can be explained as

$$\triangle^{trop} = 10^{-6} \int N^{trop} ds. \tag{3.2}$$

Dividing the delay into two components (*dry* and *wet*), the total delay can be given as

$$\triangle^{trop} = 10^{-6} \int N_d^{trop} ds + 10^{-6} \int N_w^{trop} ds. \tag{3.3}$$

This kind of dividing into components comes from practical considerations. The dry component of the tropospheric delay is precisely described by different mathematical models (for example, models of Hopfield, Niell, Saastamoinen, and others) [27]. Prediction and modeling of the wet component is complicated. The problem comes from the lack of measurement data and the instability of the troposphere (tropospheric turbulence).
The tropospheric refraction is often explained by the empiric equations [18]

$$N_{d,0}^{tropo} = \bar{c}_1 \frac{p}{T}, \quad N_{w,0}^{tropo} = \bar{c}_2 \frac{e}{T} + \bar{c}_3 \frac{e}{T^2}, \tag{3.4}$$

where $\bar{c}_1 = 77.64\ K \cdot mb^{-1}$, $\bar{c}_2 = -12.96\ K \cdot mb^{-1}$ and $\bar{c}_3 = 3.718 \cdot 10^5\ K^2 \cdot mb^{-1}$, p is atmospheric pressure in mb, T is temperature in K and e is the partial pressure of water vapor. $\bar{c}_1$, $\bar{c}_2$, $\bar{c}_3$ are empiric constants (they can have some evolution due to changes in the atmosphere). The results can be improved by measuring the real meteorological indices at the observation site. The real data are entered into some of the known refractivity models (Hopfield, Saastamoinen, etc.). It is possible to get an estimate for the dry component of the tropospheric delay with an accuracy < 1 mm if the ground surface pressure is measured with an accuracy 0.3 mb [8].

The wet component of the tropospheric delay varies remarkably (from some millimeters in polar areas and up to 40 mm in tropics). Dry component estimation needs only the air pressure and temperature at the ground surface. For the wet component, information on the relative humidity is also needed. This means that each point of measurement needs not only a GPS-receiver but also the values of 3 additional meteorological parameters – temperature, air pressure, and relative humidity.

The signal delay additionally depends on the elevation angle, having the highest values closer to the horizon. For geodetic and navigation applications it is an uncomfortable effect increasing measurement noise and inaccuracy in positioning. From the meteorological point of view the situation is more favorable – the lower the satellite above the horizon, the longer the signal path in the atmosphere and the more valuable information on the atmospheric state it may contain. In navigation, elevation angles below 15 deg are not recommended. There are restrictions in GPS-meteorological applications also coming from practical considerations. In common practice, an elevation angle cut-off of 10 degrees is used. Nevertheless, in the literature information on the observations and mapping functions down to 2 degrees over the horizon can be found [15]. The cut-off angle is one of the parameters taken into account when planning simulation experiments (and processing GPS-observations data) described in the following sections.

For elevation angles z close to 90 deg, the increase in the delay in the troposphere is proportional to $1/\cos z$. For lower angles (closer to the horizon) this simple approximation is inadequate and more sophisticated mapping functions are used (like Marini continued fraction version, Niell, Lanyi mapping function, etc.) [18, 29].

The dependence of noise in GPS-measurements is illustrated in Fig. 3.1, based on the real measurements in Tartu, Estonia. The elevation cut-off angle used is 10 degrees. The data were recorded at 10 s intervals. It is easy to notice that the lower the angle the higher the noise.

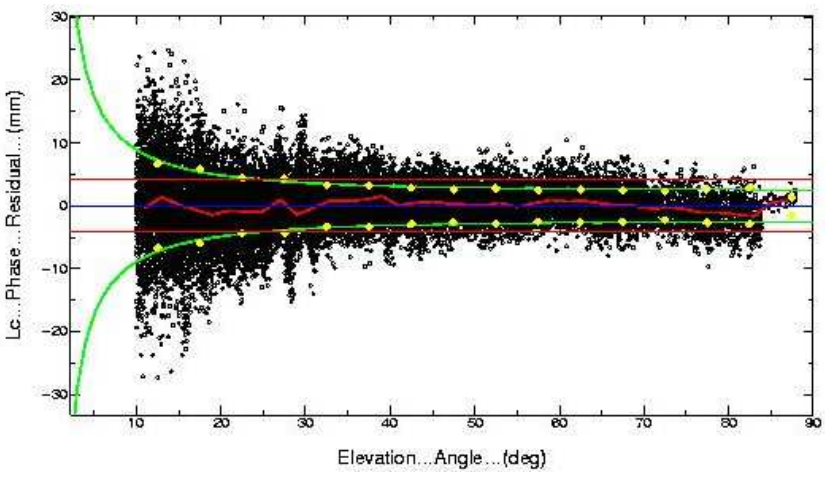

F i g. 3.1. Phase residuals growth due to the elevation angle of the GPS satellite (cut-off angle = 10 deg)

4. Estimation of tropospheric signal delays

To obtain the amount of water vapor in the atmosphere, we need a relationship between the signal delays and IPW.

The amount of integrated water in the atmosphere (in the zenith direction above the GPS-antenna) is equivalent to the height of the liquid water column. It is found by dividing the zenith integrated water vapor by the liquid water density. In a similar manner the slant water (SW) is defined as the length of an equivalent liquid water column on the ray path between the GPS-receiver i and the satellite m. SW_i^m is the Integrated Slant Water (ISW) vapor divided by the liquid water density $SW_i^m = ISW_i^m/\varrho$, where

$$ISW_i^m = \int_{rec_i}^{sat_m} \varrho_w ds. \tag{4.1}$$

The ratio of SW to the Slant Water vapor Delay (SWD) is often known as a nondimensional conversion factor Π, expressed as $\Pi = SW_i^m/SWD_i^m$. Here SWD_i^m can be derived from the STD measurements described in [10]. The IPW and SW can easily be found as $IPW = \Pi \cdot ZWD$ and $SW = \Pi \cdot SWD$ (assuming isotropic atmosphere).

$\Pi \neq$ const, its dependence on the real environmental parameters can be given [2] as

$$\Pi = \frac{10^6}{\varrho R_v [k_3/T_m + k_2']},$$

where ϱ is the liquid water density (1000 kg/m3), R_v is the specific gas constant for the water vapor (461.524 $\mathrm{Jkg^{-1}K^{-1}}$), k_3 and k_2' ($0.037 \cdot 10^5\,\mathrm{K^2/Pa}$ and 0.22 K/Pa respectively) are physical constants (by Smith and Weintraub [28]) and T_m is the mean temperature of the atmosphere. The latter is defined [7, 31, 35] as

$$T_m = \left(\int \frac{P_v}{T} dz \right) \Big/ \left(\int \frac{P_v}{T^2} dz \right),$$

where T is the temperature and P_v is the partial pressure of the water vapor. T_m can be obtained either from the surface temperature measurements or from the numerical weather models. From the surface temperature measurements Π can be estimated with an error less than 2% [1,2]. The typical value of Π is 0.15, implying that 1 mm of slant water corresponds to a SWD ∼6.5 mm. Slant water can be referred to as the equivalent amount of liquid water in units of millimeters [4].

The water-vapor-weighted atmospheric mean temperature, T_m, is a key parameter in the retrieval of atmospheric precipitable water (PW) from ground-based GPS measurements of ZPD/SPD, as the accuracy of the GPS-derived PW is proportional to the accuracy of T_m. The RMS (root mean square) error of GPS-derived PW ranges from less than 2 mm in North America to 3.7 mm in Japan. The uncertainty of 5 K in T_m corresponds to the 1.6-2.1% uncertainty in PW. T_m has also temporal and spatial variations, described in [35]. Determination of the areal numerical value for the conversion factor Π (and its variations) is a task that can be done only by long-term statistics in the area of interest.

5. Troposphere monitoring

For practical monitoring (for real reference data) a Trimble NetRS GPS-receiver was used at 58°23'30" N, 26°41'41" E, with an antenna height of 75.80 m above the reference ellipsoid.

The data is captured from December 2006 on. The data post-processing is performed by the GAMIT-software.

GAMIT-processing helps to obtain the real path/delay of the signal from each satellite to the receiver (the geometrical straight path can be calculated by the time, the satellite ephemeris, and the geographical location). The difference ("real – geometrical") gives the initial information needed for tropospheric water estimation. The GAMIT-software uses the Global Mapping Function by default developed by Boehm et al. [3] for atmospheric delays calculation. In the absence of *in situ* meteodata (common situation during modeling), the best choice of *a priori* pressure and temperature for a site comes from the "global pressure and temperature" (GPT) model. It generates surface pressure and temperature values as a function of the location and the time of the year, based on a spherical harmonic fit to 20 years of meteorological data, and reduces biases in height estimates compared with adopting standard temperature and pressure (STP) for all stations at all times [17].

To illustrate the observation process, sky-plots of the satellite trajectories are often presented (Fig. 5.1).

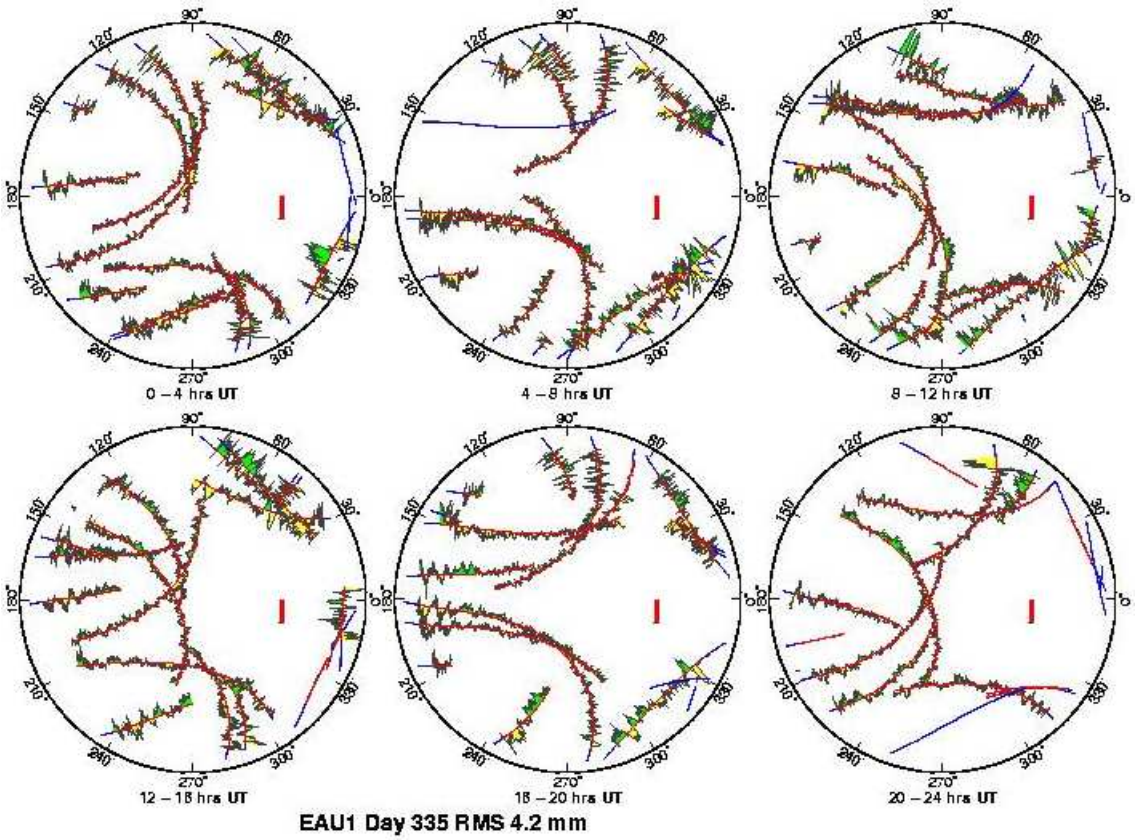

F i g. 5.1. Example of satellite trajectories, Day 335, Tartu

The plot is made for 1 day and with 4 intervals. The precise trajectories of the satellites are presented by smooth curves and the real observation phase residuals can be seen as a noise. The observer is in the middle of the circle, the North direction is on the right, East is upward and the short bar in the middle corresponds to the scale of phase residuals (in our case the bar length equals 19 mm).

Figures 3.1 and 5.1 are not the results of measurements, but they illustrate the dependence of the pre-described received signal noise on the satellite elevation angle and can

point to some technical troubles with measurements (multipath, for example). Both figures indicate that the lower the satellite is above the horizon, the more things we have to detect in the meteorological sense.

From the time differences between the real signal and the signal propagating along the shortest geometric path the integrated water content above the GPS-receivers antenna is computed. Figure 5.2 presents a 10 day interval with the corresponding evolution of the Integrated Precipitable Water, temperature, relative humidity, and air pressure in Tartu.

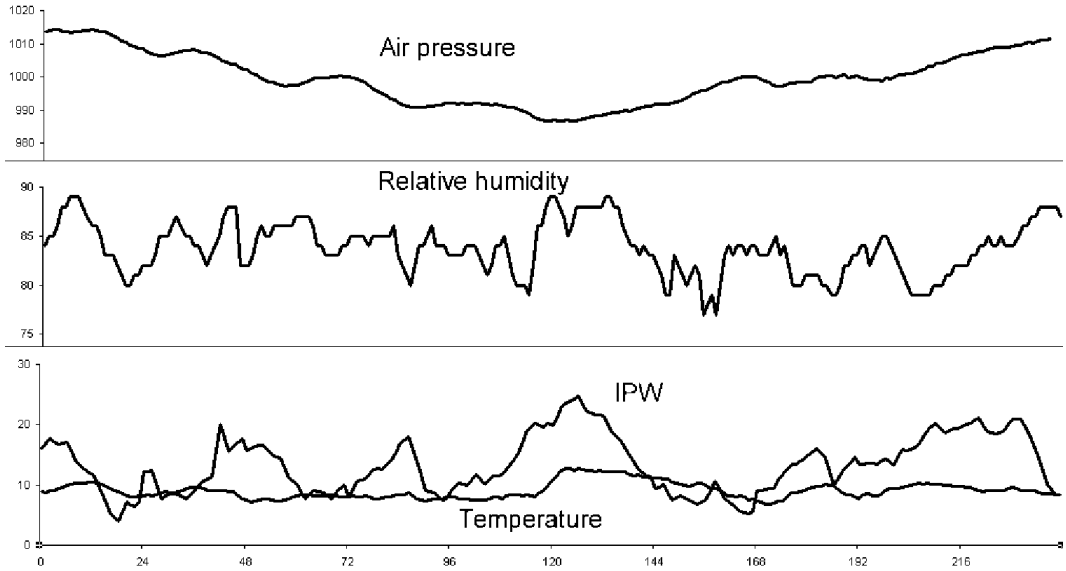

F i g. 5.2. Pressure, relative humidity, precitable water and temperature on 01-10. Dec. 2006. The horizontal resolution 1

The results presented are unsmoothed. The short-term evolution of the relative humidity at the ground level and the IPW are very unstable. It can be explained as the atmospheric turbulence, but the result contains also all undetermined noise at this stage.

6. Network of GPS-receivers and discretization of the troposphere

The installation of a hypothetical GPS-receiver network (Fig. 6.1 and Fig. 6.2) for tropospheric tomography has been modelled. Tomographic methods for obtaining the 3D distribution of tropospheric water has been the subject of numerous investigations [5, 11, 14, 25].

The idea was prompted by the conventional tomography known in medicine. The information on the ray propagation (delay or attenuation) in a certain part of the environment is obtained from different angles and later the image of the investigated constituents is reconstructed by tomographic reconstruction algorithms (often known as Radon transformations). In the model case, the delay is equivalent to the signal path (additional delay corresponds to the prolongation of the path).

From the atmospheric point of view, the GPS-signal time delays and the contribution of atmospheric water to the delays in each discrete part of the troposphere (hereafter called *voxel*) are under consideration. The discretization of the troposphere into rectangular voxels is explained in Fig. 6.3. There exist different geometrical facilities for building a system of voxels, but for the explained simulation experiment a rectangular grid was chosen as the simplest one (assuming the monitoring area relatively small). For large-scale tomography

(for areas of several hundreds of quadratic kilometres different discretization models are preferable, taking into account the Earth curvature).

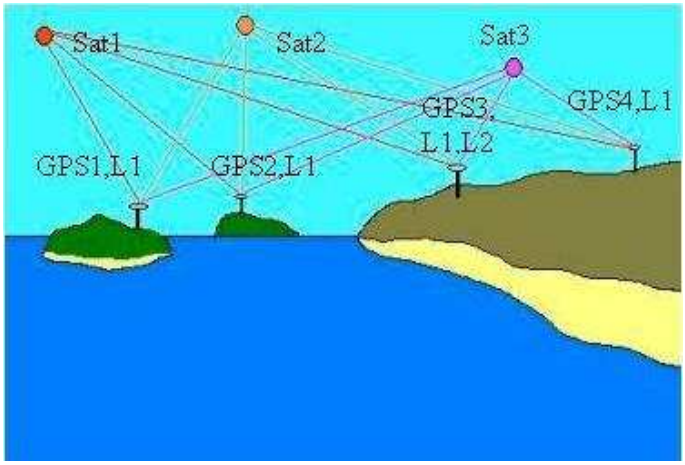

F i g. 6.1. Network of GPS receivers

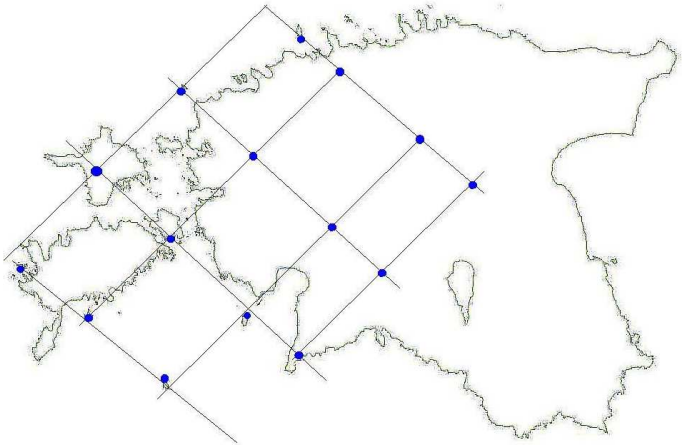

F i g. 6.2. Hypothetical network of GPS receiver in Estonia

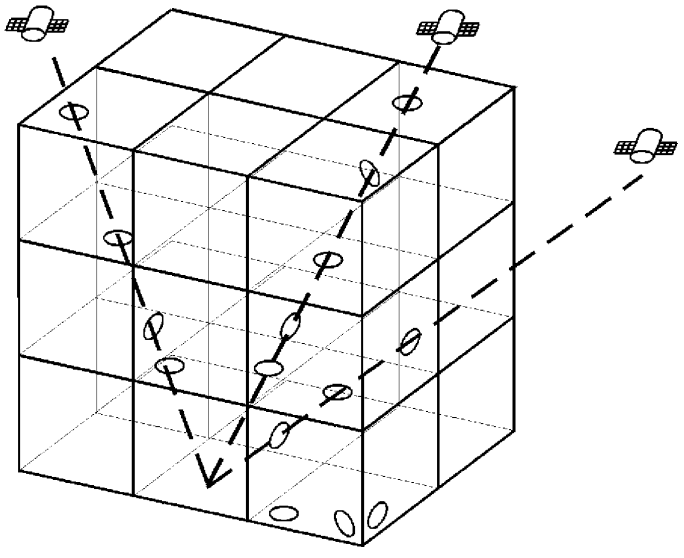

F i g. 6.3. Ray paths from satellites to a GPS-receiver through rectangular voxels

The tropospheric water is mainly distributed in a layer with a height of up to 7–10 km. The horizontal resolution of 10–40 km of the grid is known from similar experiments (station

separations $\sim$ 50 km or less recommended in the final report of the TOUGH-project [33]). Detection of water vapor takes into account all GPS-signal ray paths (where the signal has high enough quality) from the visible satellites into each location of GPS-receiver. The maximum number of ray paths is $n \cdot m$, where n corresponds to the number of satellites and m to the number of receivers. It should be noted here that n corresponds to the number of only those satellites that can be technically used in the experiment (having acceptable signal/noise ratio at a point of observation). This means that n can be smaller than the number of visible satellites (the number of usable ray paths can be reduced due to technical conditions).

The bottom facet of the voxel is rectangular. The parameters for the construction of a voxel system are the size of the horizontal grid (distance between the receivers) and the vertical step (corresponding to the number of layers in the model troposphere). The bottom of the voxel system is a tangent plane at a geographical point to the Earth as an ellipsoid. This geographical point serves as the middle point of the simulation area (middle of the virtual GPS-network).

Figure 6.4 demonstrates one simulated situation with a certain constellation of satellites, their positions related to the voxels. 144 voxels were chosen for the simulation and placed on six horizontal levels (24 voxels in each). The receivers were placed in each voxel on the ground surface, with a total number of 24. With 11 visible GPS-satellites it gives a system of 264 equations for 144 unknowns.

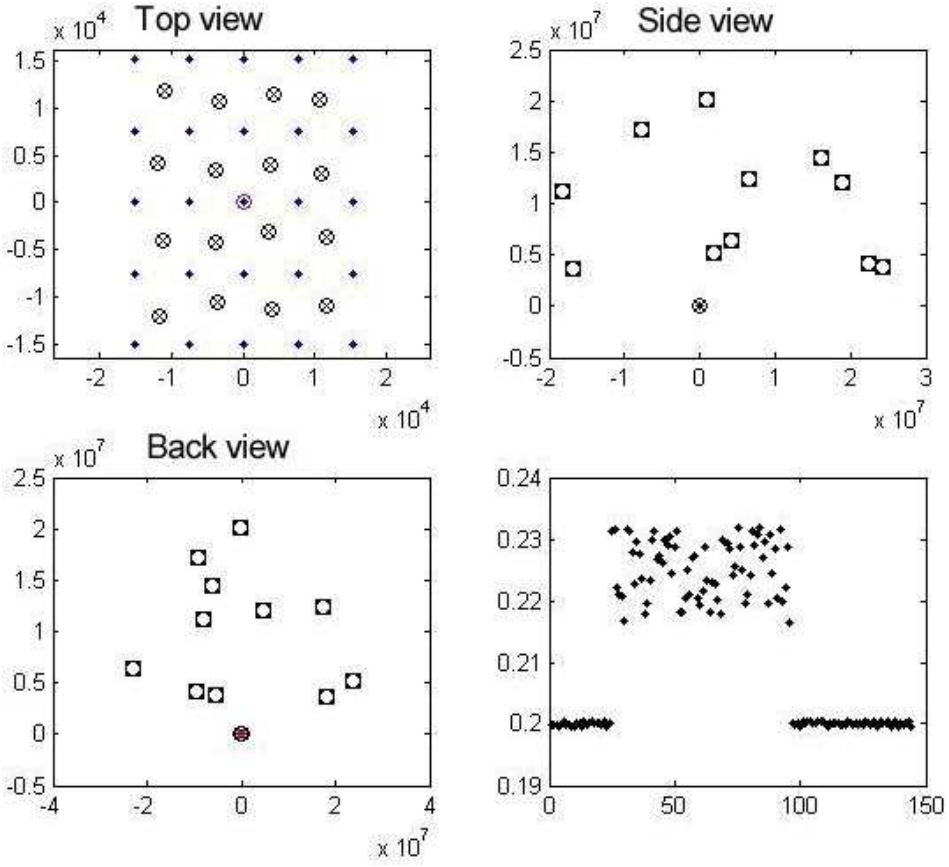

Fig. 6.4. Positions of the satellites and receivers over the area of simulated experiment and the possible prolongation of the path in voxels

In the upper row and in the left image of the lower row, circles with crosses denote the positions of GPS-receivers, squares with a circle in the middle denote the positions of

satellites, and black dots denote the vertexes of voxels. The right panel in the lower row explains the graphical image of the solution of the model system (the delays of signals in voxels).

7. The simulation model

The main problem of the tomography is to form a regular normal equation matrix which can be solved. In medicine, sencing of the human body is performed from all sides and as long as necessary to achieve a sufficiently determined numerical problem. In the GPS tomography, measurements of the atmosphere are only possible from a satellite (top) to the receivers (Earth), usually without a chance for horizontal measurements. In general, it is not possible to have enough satellites and GPS ground stations to allocate the needed amount of measurements to each voxel due to the satellites constellation, model resolution and integration time. Consequently, GPS tomography yields a difficult problem where some voxels are over-determined, but others are underdetermined from the point of view of meteorogical and tomographical information. The whole system is mixed-determined [24,32] and the inversion may become singular.

Each signal on the receiver – satellite path penetrates a certain amount of voxels. Each voxel (with water vapor) makes its individual contribution to the total delay of the signal corresponding to Eq. (3). The full path of the signal is a sum of the paths in the intercepted voxels. The model can be interpreted as a system of linear equations

$$\sum_{i=1}^{v} x_i s_{i,j} = f_j, \tag{7.1}$$

where $j = 1, \ldots, K$, K is the total number of signal paths from all visible satellites in the GPS-network at a fixed time instant, v is the total number of voxels, $s_{i,j}$ is the length of the j^{th} ray in voxel i, the x_i are considered as weights of a corresponding voxel to the slant path delay and interpreted as indicators of the PW concentration. Interpretation of the solution of the system of equations (7.1) gives the distribution of water vapor by the voxels. The differences between the geometrical shortest path and the extra path, induced by the tropospheric water (depending on the temperature, humidity and air pressure at the point of measurement), are specified by the absolute term f_i in the system of linear equations (7.1). Based on precise trajectories of the satellites obtained from IGS-service, the ray path length in each voxel is found, making the system (7.1) complete.

To solve the system of equations, the GPS-tomographic approach must fulfill some further conditions.

a) In an ideal case, at least one GPS receiver should be present in each voxel. In that way, the system is solvable. However, this network configuration is usually not possible. A topography which accounts for a good height distribution of the GPS stations contributes substantially to the quality of the solution, but unfortunately available in mountain areas only.

b) Zenith path delays on their own are not enough to construct a sufficiently determined system of equations, no matter how many delays are available (except a situation where each voxel of the lowest layer has at least one GPS receiver). With slant delays it is possible to determine a voxel, even if no GPS receiver is inside this voxel. A huge amount of slant delays with different elevation angles improves the quality of the solution significantly.

c) If the system is partially under- and partially over-determined, a technique called singular value decomposition (SVD) can be applied to diagnose and separate the under-determined part in a way, that the over-determined part of the matrix can be inverted [32]. One possibility to overcome the geometry limitations is by using the Wet Refractivity Kalman Filter described in [14].

d) Additional conditions for voxels can be used to obtain information and stabilize the system of equations. There are two possibilities. On the one hand, meteorological information obtained from independent sources can be used to specify the situation in certain voxels (microwave radiometry, weather balloons). On the other hand, a determinability of a voxel can be assured, by interpolating the refractivity between neighboring voxels.

If one or several of these conditions are fulfilled, the system of equations can be solved. Various methods exist to check the quality of the normal equation matrix. One possibility is using the Least Squares (LS) method. It can be solved also by Kalman Filter, using the prediction and correction step alternately.

The model software has two main tasks — (i) to construct the voxel system according to initial model parameters with handling of the voxel related data and (ii) monitor the signal ray paths through the voxels. Hereby it should be mentioned that the model (also the network of GPS-receivers) obtains the slant delays directly from the GPS signal phase observations, in a manner to that described in [25].

According to the satellite constellation at a certain time instant the geometrical shortest paths (Fig. 2.1) are constructed from all satellites to all of the receivers. For each signal path the intercepted voxels will be found with geometrical points of ingoing and outgoing (to fix the shortest possible ray path inside the voxel). These partial lengths are used as coefficients in system (7.1). Each ray will penetrate only a minor part of voxels and the situation changes at each time step.

The simulation of monitoring consists of the generation of initial data for a certain mathematical model and the data processing related to a specific scenario. The synthetic data consist of the outputs of GPS-receivers (including both (i) the data sent by a satellite and (ii) the data generated by a receiver).

The *first category* represents mostly the positions of the satellites and the time parameters of atomic clocks. These data consist of the GPS-satellite navigation message and can also be obtained from GPS Ground Control Stations or some public databases via internet. The *second category* consists of data about the time instants the signal was received (receiver time), the carrier phase, the position of satellites (from the receivers point of view) and some supporting information.

The simulation program compiled on the basis of the mathematical model is responsible for the generation of a situation as realistic as possible. The model situation must be described by the real geographical location and the real constellation of GPS-satellites at a certain time instant. Based on this information additional analysis is performed to find suitable locations for GPS-receivers in the monitoring network. The criterion is the solution of system (7.1) — the result must be realistic in the meteorological sense.

The simulation helps to determine under which initial conditions system (7.1) can be resolved and when the result is reliable.

8. Error management and filtering of initial data

Although the GPS-measurements are believed to be extremely accurate mostly for every application, they can exhibit significant errors depending on the environmental conditions and the technical dacilities of experiments. The GPS error analysis (one can find from [26] and many other handbooks) is out of the scope of current modeling experiment.

From the modeling point of view and geodetic accuracies the results are mostly affected by orbit errors and clocks drift.

Assimilation of the results into NWP models needs accuracies better than 2 mm of PWV (Precipitable Water Vapor) within 1 h of data collection [16]. For now-casting (often referred to as the weather forecasting in the 0–12 hrs timeframe) the TOUGH project report [34] recommends a time resolution of nearly real time (NRT) GPS data as high as 2–4 observations/hour with an update every hour, with a potential for faster updates in the future.

The first obstacle for geodetic data processing is related to the delayed availability of GPS-satellites precise orbits (the errors in orbit data affect directly the estimation of delays). For real- and near real time applications, only predicted or Ultra Rapid (delivered twice a day, containing 24 hrs of "real" orbit data from the International GPS Service (IGS) hourly network and the rest 24 hrs are predicted) products can be used. Improvement can be achieved by the sliding-window technique [12].

The orbit errors are systematic (except for the occasions of Sun bursts), therefore they are easier to handle. Receiver clock errors can be eliminated mainly by the double-differencing method. Systematic errors can be eliminated by combining and comparing different data of observations.

Atmospheric tomography (and the related modeling) has additionally some specific sources of errors that cannot be ignored. The *first* source is related to the voxels (the meaning of the term will be given later), not giving any information (because of not being intercepted by any signal ray) and the *second* one is related to the real data acquisition at the point of measurement (sudden malfunction of some of the sensors or loss of the data).

The *first* category of problems is expected to be smoothed by Kalman Filtering (KF). KF and smoothing have also been used in the GPS-campaign in Onsala [11]. The successful exploitation of KF or its modifications [19, 21, 22, 37] is not always straightforward due to the limitations coming from the receiver network geometry. KF needs also the observability and controllability conditions to be satisfied [13], otherwise the algorithm will not converge. The Wet Refractivity Kalman Filter [14] can be used as one of the possibilities to resolve poor geometry.

The *second* category of errors is overcome by using the paradigm of *agents*. By this concept each node of the network of GPS-receivers is considered as an autonomous proactive agent, with the main task to capture the data on GPS-observations and 3 additional meteoparameters. Additionally, each node (agent) is responsible for the data link with the central data processing unit. If, for example, one meteoparameter (let's say the ground surface temperature) is missing, then it can be requested from the adjacent agents, the result will be interpolated to the malfunctioning node and "complete" data will be sent to the central unit. This makes it technically possible to distribute some operational tasks to the agents in the nodes leaving more computational resources to the data processing.

The random measurement errors are also processed by KF. The KF addresses the general problem of trying to estimate the state of a discrete-time controlled process governed by the

linear stochastic difference equation

$$X_k = AX_{k-1} + w_{k-1} \tag{8.1}$$

and measurement

$$Z_k = HX_k + v_k. \tag{8.2}$$

Here X and Z are the vectors of n- and m-dimensional real Euclidean space respectively. The random variables w_k and v_k represent the process noise and the measurement noise (respectively). They are assumed to be independent of each other and auto-independent, white, with normal probability distributions $P(w) \approx N(0, Q)$ and $P(w) \approx N(0, R)$. In practice, the process noise covariance Q and measurement noise covariance R matrices might change at each time step or measurement, however here assumed constant. The $n \times n$ matrix A in the difference equation (8.1) relates the state at the previous time step $k-1$ to the state at the current time step k, in the absence of either a driving function or process noise. Note that in practice A might change with each time step, but here we assume it to be constant. The $m \times n$ matrix H in the measurement equation (8.2) relates the state to the measurement Z_k. In practice H might change at each time step or measurement, but here in the model case we assume it also constant.

KF is not applied to the model yet as all the data sets in use are generated or extrapolated. Exploiting KF in further experiments is inevitable, when the modeling data is assimilated with real measurements.

Finding the best modification of KF is one of the challenges of the modeling, as numerical precision and stability is counterbalanced with computational load, directly related to the applicability of the monitoring concept and sensor network.

Acknowledgment. This paper was supported by the Estonian Science Foundation, grant No. 7097.

References

1. M. Bevis, S. Businger, T. A. Herring, C. Rocken, R. A. Anthes, and R. H. Ware, *GPS meteorology: Remote sensing of atmospheric water vapor using the Global Positioning System*, J. Geophys. Res., **97** (1992), pp. 15, 787–15, 801.

2. M. Bevis, S. Businger, S. Chiswell, T. A. Herring, R. A. Anthes, C. Rocken, and R. H. Ware, *GPS meteorology: Mapping zenith wet delays onto precipitable water*, J. Appl. Meteorol., **33** (1994), pp. 379–386.

3. J. Boehm, A. Niell, P. Tregoning, H. Schuh, *Global Mapping Function (GMF): A new empirical mapping function based on numerical weather model data*, Geophysical Research Letters, **33** (2006), L07304, doi:10.1029/2005GL025546.

4. J. Braun, C. Rocken, and R. Ware, *Validation of line-of-sight water vapor measurements with GPS*, Radio Science, **36** (2001), pp. 459–472.

5. J. Braun and C. Rocken, *Water vapor tomography within the planetary boundary layer using GPS*, Proc. of the International Workshop on GPS Meteorology, GPS Meteorology: Ground-Based and Space-Borne Applications (Tsukuba, Japan, January 14–17, 2003).

6. G. Chen and T. Herring, *Effects of atmospheric azimuthal asymmetry on the analysis of space geodetic data*, J. Geophys. Res., **102** (1997), pp. 20489–20502.

7. J. Davis, T. Herring, I. Shapiro, A. Rogers, and G. Elgered, *Geodesy by radio interferometry: Effects of atmospheric modeling errors on estimates of baseline length*, Radio Sci., **20** (1985), pp. 1593–1607.

8. J. P. Duan, M. Bevis, P. Fang et al., *GPS Meteorology: Direct Estimation of the Absolute Value of Precipitable Water*, Journal of Applied Meteorology, **35** (1996), no. 6, pp. 830–838.

9. P. Elosegui and J. L. Davis, *Accuracy assessment of GPS slant-path determinations*, in: *Proceedings of the International Workshop on GPS Meteorology, Tsukuba, Japan, 1417 Jan 2003* (T. Iwabuchi and Y. Shoji, eds.) (2004).

10. R. Eresmaa and H. Järvinen, *An Observation operator for ground based GPS slant delays*, Tellus A, **58** (2006), no. 1, pp. 131–140.

11. A. Flores, L. P. Gradinarsky, P. Elosegui, G. Elgered, J. L. Davis, and A. Rius, *Sensing atmospheric structure: tropospheric tomographic results of the small-scale GPS campaign at the Onsala Space Observatory*, Earth Planets Space, **52** (2000), pp. 941–945.

12. J. Foster, M. Bevis, and S. Businger, *GPS Meteorology: Sliding-Window Analysis. Journal of Atmospheric and Oceanic Technology*, AMS, **22** (2005), pp. 687–695.

13. A. Gelb. (ed.), *Applied Optimal Estimation*, MIT Press, Cambridge, MA, 1984.

14. L. G. Gradinarsky, *Sensing Atmospheric Water Vapor Using Radio Waves*, Ph.D. thesis, Chalmers University of Technology, Technical report No. 436 (2002).

15. J. Guo and R. B. Langley, *A new Tropospheric Propagation Delay Mapping Function for Elev. Angles Down to 2 deg*, Proceedings of ION GPS/GNSS 2003, 16th International Technical Meeting of the Satellite Division of The Institute of Navigation, Portland, OR, 9–12 September 2003, pp. 386–396.

16. S. I. Gutman and S. G. Benjamin, *The role of ground-based GPS meteorological observations in numerical weather prediction*, GPS Solutions, **4** (2001), pp. 16–24.

17. T. A. Herring, R. W. King and S. McClusky, *GAMIT Reference Manual*, Release 10.3, Department of Earth, Atmospheric, and Planetary Sciences, MIT, 2006.

18. B. Hofmann-Wellenhof, H. Lichtenegger, and J. Collins, *GPS Theory and Practice*, Springer-Verlag Wien, New York, NY, USA, fifth edition, 2001.

19. R. E. Kalman, *A new Approach to Linear Filtering and Prediction Problems*, Transaction of the ASME J.of Basic Engineering, March 1960, pp. 35–45.

20. J. Klobuchar, *Ionospheric effects in GPS*, in: *Global Positioning System: Theory and applications* (B. Parkinson and J. Spilker, eds.), **I**, Chapter 12, 1996.

21. A. A. Lange, *Statistical calibration of observing systems*, Academic Dissertation, FMI, Helsinki, 1999.

22. A. A. Lange, *Simultaneous Statistical Calibration of the GPS signal delay measurements with related meteorological data*, Physics and Chemistry of the Earth, Part A: Solid Earth and Geodesy, **26** (2001), no. 6–8, pp. 471–473.

23. P. Miidla, K. Rannat, and P. Uba, *Simulation of the Tropospheric Water Vapor Distribution Monitoring*, Proceedings of the I3M International Mediterranean Modelling Multiconference, EMSS 2005, Marseille, France, October 20–22, 2005, pp. 223–228.

24. W. Menke, *Geophysical Data Analysis: Discrete Inverse Theory*, International Geophysics Series, **45**, Academic Press.

25. T. Nilsson, *Assessment of Tomographic Methods for Estimation of Atmospheric Water Vapor Using Ground-Based GPS*, Thesis for the degree of Licentiate of Engineering, Chalmers University of Technology, 2005.

26. B. W. Parkinson and J. J. Spilker, *Global Positioning System: Theory and Applications*, American Institute of Aeronautics and Astronautics, **1** (1996).

27. S. M. Shrestha, *Investigations into the Estimation of Tropospheric Delay and Wet Refractivity Using GPS Measurements*, A Thesis in partial fulfilment of the requirements for the degree of master of science, Calgary, Alberta, 2003.

28. E. Smith and S. Weintraub, *The constants in the equation for atmospheric refractive index at radio frequencies*, Proc. IRE, **41**(1953), pp. 1037–1053.

29. J. J. Spilker Jr., *Tropospheric effects on GPS*, in: *Global Positioning System: Theory and applications* (B. Parkinson, J. Spilker, eds.) , **1** (1996), Chapter 13.

30. B. Stoew, P. Jarlemark, J. Johansson, and G. Elgered, *Real-time processing of GPS data delivered by SWEPOS*, Phys. Chem. Earth (A) **26** (2001), pp. 493–496.

31. P. Tregoning, *Accuracy of absolute precipitable water vapor estimates from GPS observations*, Journal of Geophys. Res., **103** (1998), pp. 28701–287109.

32. M. Troller, *GPS based Determination of the Integrated and Spatially Distributed Water Vapour in the Troposphere*, Diss. ETH No. 15513, 2004.

33. H. Vedel et al, *Final report for the TOUGH project*, in: *Targeting Optimal use of GPS Humidity Measurements in Meteorology, EVG1-CT-2002-00080, 6th Periodic Report, 1 February 2003 31 January 2006 (2006a), Section 6* (H. Vedel , Co-ordinator). http://tough.dmi.dk

34. H. Vedel et al. *GPS Data Recommendations for European Numerical Weather Prediction*, in: *Targeting Optimal use of GPS Humidity Measurements in Meteorology, Deliverable D73 (2006b)* (H. Vedel, Co-ordinator). http://tough.dmi.dk

35. J. Wang, L. Zhang, and A. Dai, *Global estimates of water-vapor-weighted mean temperature of the*

atmosphere for GPS applications, Journal of Geophysical Research, **110** (2005), D21101, doi:10.1029/2005JD006215.

36. R. Ware, C. Alber, C. Rocken, and F. Solheim, *Sensing Integrated Water Vapor along GPS Ray Paths*, Geophys. Res. Lett., **24** (1997), pp. 417–420.

37. G. Welch and G. Bishop, *An Introduction to the Kalman Filter*, University of North Carolina. Shapel Hill, TR 95-41, 2003.

38. G. Xu, *GPS. Theory, Algorithms and Applications*, Springer Verlag Berlin, Heidelberg, 2003.